ADVANCED HEALTHCARE MATERIALS
www.advhealthmat.de

Effects of Mesenchymal Stem Cell-Derived Paracrine Signals and Their Delivery Strategies

*Calvin Chang, Jerry Yan, Zhicheng Yao, Chi Zhang, Xiaowei Li, and Hai-Quan Mao**

Mesenchymal stem cells (MSCs) have been widely studied as a versatile cell source for tissue regeneration and remodeling due to their potent bioactivity, which includes modulation of inflammation response, macrophage polarization toward proregenerative lineage, promotion of angiogenesis, and reduction in fibrosis. This review focuses on profiling the effects of paracrine signals of MSCs, commonly referred to as the secretome, and highlighting the various engineering approaches to tune the MSC secretome. Recent advances in biomaterials-based therapeutic strategies for delivery of MSCs and MSC-derived secretome in the form of extracellular vesicles are discussed, along with their advantages and challenges.

1. Introduction

Mesenchymal stem cells (MSCs) or mesenchymal stromal cells are increasingly recognized as a promising therapeutic over the past few decades.[1] The International Society for Cellular Therapy (ISCT) initially defined MSCs as fibroblast-like multipotent adult stem cells with the capacity to self-renew and are plastic-adherent under standard culture conditions, positive (≥95%) for cluster of differentiation (CD) markers CD105, CD73, and CD90, while negative (≤2%) for CD45, CD34, CD14/CD11b, CD79α/CD19, and human leukocyte antigen (HLA)-DR isotype, and able to differentiate into osteoblasts, adipocytes, and chondrocytes.[2] Cells with similar properties have also been identified from other tissues including adipose tissue, umbilical vein, dental pulp, and synovial membrane.[3–6] These cells share the common features of multipotency, ease of expansion, and versatile bioactivity profile. Significant progress has been made to expand the therapeutic effects of MSCs in different disease models and regenerative repairs. Despite of over 1100 clinical trials testing the therapeutic benefits of MSCs from different sources, treatment outcomes varied significantly. The inconsistency highlights the need for a better examination of the underlying mechanisms behind MSC-based regeneration and repair of MSC therapeutics. Increasing evidence suggests that the original definition of cell source and surface markers is not indicative of therapeutic outcomes.[7] Recently, ISCT extended their definition of MSCs to be supplemented by tissue-source origin of cells to highlight tissue-specific properties, demonstrating stemness from both in vitro and in vivo data, and associated with functional activities that are not generally defined but rather informed by the intended therapeutic mode of actions.[8] Functional activities and therapeutic applications of MSCs are most commonly attributed to two main mechanisms. The first relies on the differentiation, engraftment, and integration of the exogenous MSCs into the host tissue during the repair process. In the hematopoietic microenvironment, for example, MSCs in the bone marrow can give rise to osteoblasts, adipocytes, and stromal fibroblasts. Through the transplantation of green fluorescent protein-transduced human MSCs in nonobese diabetic/severe combined immunodeficiency (NOD/SCID) mice, Muguruma et al. demonstrated direct visual evidence of engraftment in the murine bone marrow in 10 weeks, including differentiation into osteoblasts and osteocytes, and in rare occasions, CD34 and CD31 positive endothelial cells.[9] The second mechanism primarily relies on the paracrine signaling from the transplanted cells, which acts through the secretion of signaling cues to induce host tissue regeneration.

The efficacy of MSC therapy, regardless of the mechanism and delivery approaches, must consider the homing, adhesion, survival, retention, immunomodulation, angiogenesis, engraftment, and integration of transplanted MSCs at the tissue repair site. Upon delivery of MSCs, either via homing or by direct injection, further complications include the inflammation,

C. Chang, J. Yan, Prof. H.-Q. Mao
Department of Biomedical Engineering, School of Medicine
Johns Hopkins University
Baltimore, MD 21205, USA
E-mail: hmao@jhu.edu
C. Chang, J. Yan, Z. Yao, Dr. C. Zhang, Prof. H.-Q. Mao
Translational Tissue Engineering Center
Johns Hopkins School of Medicine
Baltimore, MD 21287, USA
C. Chang, J. Yan, Z. Yao, Dr. C. Zhang, Prof. H.-Q. Mao
Institute for NanoBioTechnology
Johns Hopkins University
Baltimore, MD 21218, USA
Z. Yao, Dr. C. Zhang, Prof. H.-Q. Mao
Department of Materials Science and Engineering, Whiting School of Engineering
Johns Hopkins University
Baltimore, MD 21218, USA
Dr. X. Li
Mary and Dick Holland Regenerative Medicine Program
and Department of Neurological Sciences
University of Nebraska Medical Center
Omaha, NE 68198, USA

The ORCID identification number(s) for the author(s) of this article can be found under https://doi.org/10.1002/adhm.202001689

The author biographies for this article were added on 15 January 2021 after original online publication.

DOI: 10.1002/adhm.202001689

hypoxia in the local microenvironment, which leads to challenges of MSC engraftment and integration to the host tissue. The interaction between MSCs and extracellular matrix (ECM) at the target tissue is critical to cell survival and retention; and the lack of cell adhesion or MSC–ECM interaction leads to an apoptotic process known as anoikis. As a result of reduced anchorage-dependent signaling, downregulated phosphoinositide 3-kinase/protein kinase B (PI3K/Akt) and mitogen-activated protein kinase/extracellular-signal-regulated kinase (MEK/ERK) pathways from integrin receptor binding contributes to the low percentage of MSC engraftment after transplantation.[10,11] Strategies to address these challenges associated with the delivery of MSCs are central to successfully harness the full potential of MSCs for clinical applications.

Microenvironment properties can influence the deposition of proteins and ECM remodeling components that are crucial in establishing the MSC niche. In a study by Loebel et al., nascent proteins deposited through MSC-hydrogel interaction were influenced by matrix stiffness with the focal adhesion sites contributing to production of fibronectin, laminin, collagen, and paxillin. This can further influence MSC mechano-signaling through Yes-associated protein and transcriptional coactivator (YAP/TAZ) pathway to result in MSC differentiation.[12] Of the few studies that quantified efficiency of MSC engraftment in vivo, poor survival outcomes were observed, thus challenging the classical paradigm of differentiation and engraftment of exogenous MSCs leading to regeneration of the damaged tissue.[13–20] The MSCs that were reported to engraft lacked in sufficient quantity and duration of engraftment to directly cause the improvements in tissue repair.[21–25] Recent efforts have now been directed to examining the paracrine activity of transplanted MSCs and its effect on cellular populations recruited to the local tissue, as well as longer-term regenerative responses.

2. The MSC Secretome

The paradigm shift toward paracrine signaling as the primary mechanism of MSC therapeutic efficacy has led to a growing focus toward the regenerative and immunomodulatory potential of the conditioned medium after MSC culture, which contains growth factors, cytokines, microRNA (miRNA), and other small molecular weight signal cues. These MSC-secreted factors within conditioned media, termed the MSC "secretome," has been correlated with a majority of the therapeutic benefits provided by MSCs.[26–28] Various studies using the MSC secretome have demonstrated therapeutic potential in prevalent injury models.[29–31] Characterization of the MSC secretome in different applications ranging from cartilage regeneration to cardiovascular and other microenvironments has been performed using standard techniques such as enzyme-linked immunosorbent assay (ELISA), liquid chromatography-mass spectrometry (LC-MS), and proteomics-based profiling. The components of the secretome can vary drastically in both composition and concentration, depending on various cellular and preparation parameters.[32–35] Due to the highly versatile nature of MSCs, the preferred secretome for each application can be tailored; therefore the therapeutic outcomes can be manipulated through intrinsic as well as extrinsic factors such as biomaterials.

3. Characterization of MSC Secretome for Various Applications

The MSC secretome is mainly characterized as anti-inflammatory, angiogenic, and immunomodulatory, although other activities such as antifibrosis, neuroprotection, and promoting cell proliferation have also been reported (**Table 1**). A common group of factors identified in the MSC secretome among MSCs from different sources includes vascular endothelial growth factor (VEGF), basic fibroblast growth factor (bFGF), and hepatocyte growth factor (HGF).[28,34,36–38] Other angiogenic and immunomodulatory growth factors and cytokines include stromal cell-derived factor 1 (SDF-1), transforming growth factor β1 (TGF-β1), insulin-like growth factor 1 (IGF-1), platelet-derived growth factor (PDGF), and interleukin 6 (IL-6). Additional components, particularly miRNAs, also play a major role in shaping the unique characteristics of each secretome. The most notable ones are miR-23, miR-29, and miR-125b, all of which are considered to target genes that regulate vascular development, angiogenesis, and overall regulation of cell growth.[39–42] The concentration of each molecule within the secretome may vary across different preparations.[43–46] These findings not only highlight the importance to better characterize the secretome for quality control purpose, but also reveal the need to understand the optimal secretome profile for a specific application and identify the specific mechanistic pathways in regeneration of different tissue types. For example, the secretome of MSCs during cartilage regeneration or chondrogenesis is characterized by high levels of TGF-β1, tissue inhibitor of metalloproteinase 3 (TIMP-3), and matrix metalloproteinase 13 (MMP13)[35,47–51] Among the secretome components, fibroblast growth factor-1 (FGF-1) and PDGF, besides their angiogenic properties, also contribute to the proliferation of chondrocytes.[52] The miRNA components miR-204, miR-211, miR-337 are correlated with preventing cartilage degradation and promoting chondrogenesis.[42,44]

In cardiovascular tissue repair, it is crucial to minimize fibrotic scarring in order to prevent stiffening of the cardiac tissue and thus maintain tissue function.[26,29,52] Natural antagonists of MMP-9 and IL-6, including TIMP-3, interleukin 10 (IL-10), indoleamine 2,3-dioxygenase (IDO), and prostaglandin E2 (PGE_2), are upregulated during myocardial infarction (MI) and result in fibrotic scarring. These MSC-secreted antifibrotic antagonists have been utilized to reduce the fibrotic scarring that is generated in the MI microenvironment.[29,53] In addition, MSC secretome components miR-21, miR-130a, miR-210, and miR-214 have been associated with improved angiogenesis or antiapoptotic effects, as well as reduction in infarct size.[54–58] The MSC-mediated antifibrotic approach is also highly relevant to neural regeneration, in addition to promoting neuronal differentiation and axonal outgrowth. Secretome components such as TGF-β1, IL-10, and miR-124 are responsible for reducing neuroinflammation while miR-9, brain-derived neurotrophic factor (BDNF), nerve growth factor (NGF), and glial cell-derived neurotrophic factor (GDNF) are important for neuronal growth.[38,40,44]

MSCs have been extensively studied in wound healing to promote hemostasis, angiogenesis, cell proliferation, reduce inflammation, and accelerate wound closure. MSC-secreted factors, such as PDGF, and an array of miRNAs have been identified with specific roles in angiogenesis (miR-21), re-epithelialization

Table 1. Key secretome components involved in MSC-induced biological functions.

Biological function[a)]	Key growth factors and cytokines	Key micro-RNAs (miRNAs)
Antiapoptosis	VEGF, bFGF, G-CSF, HGF, IGF-1, STC-1, IL-2, IL-6, IL-9	miR-25, miR-214
Angiogenesis	VEGF, bFGF, MCP-1, PDGF, HGF, IL-6, IL-8	miR-21, miR-23, miR-27, miR-126, miR-130a, miR-210, miR-378
Immunomodulation	IDO, HGF, PGE_2, TGF-β1, TSG-6, IL-7, IL-10, IL-19, IL-38	miR-21, miR-146a, miR-375
Chemoattraction	IGF-1, SDF-1, VEGF, G-CSF, MCP-1, IL-8, IL-16	
Proliferation	VEGF, bFGF, HGF, IGF-1, LIF, MCP-1, PGE_2, SDF-1, PDGF, IL-2	miR-17
Antifibrosis	HGF, PGE_2, IDO, IL-10	miR-26a, miR-29, miR-125b, miR-185
Neuroprotection	BDNF, NGF, GDNF	miR-9, miR-124

[a)] Abbreviations: VEGF (vascular endothelial growth factor), bFGF (basic fibroblast growth factor), G-CSF (granulocyte colony-stimulating factor), HGF (hepatocyte growth factor), IGF-1 (insulin-like growth factor-1), STC-1 (stanniocalcin-1), MCP-1 (monocyte chemoattractant protein-1), PDGF (platelet-derived growth factor), IDO (indoleamine 2,3-dioxygenase), PGE_2 (prostaglandin E_2), TGFβ1 (transforming growth factor beta1), TSG-6 (tumor necrosis factor-inducible gene 6), SDF-1 (stromal cell-derived factor 1), LIF (leukemia inhibitory factor), BDNF (brain-derived neurotrophic factor), NGF (nerve growth factor), GDNF (glial cell-derived neurotrophic factor).

(TIMP-1, HGF, bFGF, miR-21, miR-31, and miR-483), and modulation of inflammation-related interleukin-1 receptor antagonist (IL-1Ra), miR-21, miR-155, and miR-146.[44,59–64] The secretome has been shown to activate the appropriate signaling cascades resulting in the subsequent proliferative, angiogenic, and anti-inflammatory phases of wound healing. An MSC secretome has also been utilized to accelerate cutaneous wound healing through proliferation of endothelial cells, antiapoptotic effects, and reduction of inflammation.[65] As these phases of wound healing are largely sequential with slight overlap in each stage, an ideal presentation of MSC-secreted factors should match this healing and repair process over time.

4. Engineering MSC Secretome

The secretome transferred between the MSCs and other native cells in the target tissue microenvironment through the release of extracellular vesicles (EVs), which includes microvesicles and exosomes. Treatments with EVs are considered safer for therapeutic applications compared to MSC therapy; and EVs can be efficiently delivered due to their small sizes ranging from 30 to 150 nm.[26,27] There are many factors involved in choosing the appropriate cell source for EV production that can significantly influence the bioactivity profile of the secretome, such as the origin, age, and culture conditions of the MSCs.[66,67] One study comparing bone marrow-derived MSC (BM-MSCs), Wharton's jelly-derived MSCs (WJ-MSCs), and adipose tissue-derived MSC (ADSCs) found at least 20-fold higher VEGF-A secretion in BM-MSCs and ADSCs compared to WJ-MSCs, while WJ-MSCs upregulated at least threefold expression of HGF compared to the other cell sources.[43] Besides these cell-intrinsic factors, numerous extrinsic factors can be tuned to condition MSCs and thus tailor the secretome for specific applications. The major approaches that have been explored to condition MSCs and engineer the secretome include inducing hypoxia, treatment with bioactive agents or growth factors, and modulating cell–cell and ECM interactions in the MSC culture (**Table 2**).

4.1. Inducing Hypoxia in MSC Culture

Hypoxia, which refers to conditions where the oxygen tension is significantly lower than the normal physiological oxygen concentration, has been utilized during cell culture to enhance the angiogenic effects of the MSC secretome. As the oxygen tension is relatively low under most physiological microenvironments, hypoxic conditions are also suggested to better promote in vivo efficacy than normal oxygen condition.[68–70] While hypoxic microenvironments are more commonly studied in cancer progression, preconditioning MSCs in hypoxic conditions is safe and nononcogenic both in vitro and in vivo.[71] Culturing MSCs under hypoxia promotes the proliferation and migration of MSCs and boosts the bioactivities of the secretome, as evidenced by increasing levels of VEGF, NGF, and BDNF as well as immune mediators such as IL-6, IL-15, and IL-1β.[4,43,71–74] The effect of hypoxic preconditioning on growth factor secretion can vary between different MSC sources or specific environmental cues (**Figure 1**). As shown by Petrenko et al., BM-MSCs cultured under hypoxia condition show a greater level of VEGF, whereas ADSCs give a higher level of NGF, suggesting that hypoxic preconditioning on growth factor secretion may vary between MSCs from different sources due to differences in sensitivity to metabolic conditioning.[43]

4.2. Treating MSCs with Bioactive Agents

Supplementing MSC culture media with specific bioactive agents can also condition MSCs effectively and thus tune the EV components. Deferoxamine (DFO) is most commonly prescribed to treat acute iron poisoning due to its ability to chelate iron. This activity can be utilized to promote angiogenesis and prevent inhibition of hypoxia-inducible factor 1-alpha (HIF-1α) hydroxylation; the treatment of MSCs with DFO elicits effects similar to hypoxia with upregulation of angiogenic growth factors like HIF-1α and VEGF, correlating with an increase in early vascularization and tissue viability, although its effects on inflammation is not as clearly defined.[75–77] Other agents, like valproic acid (VPA), have been utilized to enhance anti-inflammatory activity with an increase in IL-10 while attenuating IL-6 expression.[78–80] A common approach is to directly introduce the appropriate chemokines as preconditioning to take advantage of the MSC feedback system between regeneration and the immunomodulatory response. The introduction of an inflammatory chemokine, most commonly interferon gamma (IFN-γ), during culture evokes an enhanced anti-inflammatory response from MSCs, increasing expression of IDO and HLA

Table 2. Various approaches to modulate MSC secretome.

Approach/method[a)]	Cell type	Additional conditions	Outcomes
Inducing physiological stress, e.g., culturing cells at constant agitation or under a hypoxia condition	BM-MSCs	Stirred suspension via bioreactor	Upregulated two- to threefold expression of BDNF, VEGF, NGF, and 30-fold expression of IGF-1 compared to static culture.[127]
	Umbilical-derived MSCs	5% O_2	Upregulated 1.5–2.5-fold expression of VEGF, BDNF, HGF.[128]
	ADSCs	1% O_2	Upregulated 2.5-fold expression of VEGF and twofold expression of FGF.[43]
	ADSCs and BM-MSCs	5% O_2	Upregulated 1.5-fold expression of VEGF-A in BM-MSC and fourfold expression of NGF in ADSC.[74]
Employing extrinsic signals, e.g., stimulating cells with bioactive agents	BM-MSCs	TNF-α	Upregulated 1.5–2-fold expression of HGF, SDF-1, VEGF, and immunomodulatory cytokine IL-6.[84]
	BM-MSCs	Li-VPA	Up-regulated two- to fourfold expression of NDNF, IGF-1, BMP-6, and anti-inflammatory cytokine IL-19. Upregulated tenfold expression of MMP-17.[62]
	ADSCs	DFO	Upregulated two- to fivefold expression of VEGF, SDF-1, and immunomodulatory cytokine IL-6.[129]
	BM-MSCs	IFN-γ + TNF-α	Upregulated sevenfold expression of anti-inflammatory cytokine IL-10.[81]
Enhancing cell–cell interaction, e.g., culturing cells in the spheroid form	BM-MSCs	Spheroids	Upregulated up to 500-fold expression of TSG-6 and 20-fold STC-1 expression in all spheroids tested.[88]
	ADSCs	Spheroids	Upregulated 900-fold expression of anti-inflammatory cytokine IL-10 and 40-fold expression of TSG-6.[90]
	Umbilical-derived MSCs	Spheroids	Upregulated 250-fold expression of VEGF, downregulated threefold, 250-fold, and 15-fold expression of bFGF, SDF-1, and HGF, respectively.[87]
	Umbilical-derived MSCs	Spheroids	Upregulated fivefold, 80-fold, 15-fold, and fivefold expression of HGF, VEGF-A, FGF, and TGFb, respectively.[130]
	ADSCs	Spheroids	Upregulated 1.5–3-fold expression of VEGF, SDF-1, and HGF.[131]
	Umbilical-derived MSCs	Spheroids	IL-7 and VEGF only detected from secretion of spheroid compared to 2D culture, upregulated one- to twofold expression of SDF-1, and immunomodulatory cytokine IL-6.[132]
Modulating cell-substrate interaction, e.g., tuning ECM conditions	BM-MSCs	ECM stiffness ligand-density	Stiffness, stress relaxation, and ligand density of substrate coupled together influenced more than 30% of the 1500 genes examined. An 18 kPa substrate with a low ligand-density showed 1.25–2.5-fold higher expression of SDF-1α and IGF-1 compared to a 3 kPa substrate with a low ligand-density and a 18 kPa substrates with a high ligand-density.[91]
	BM-MSCs	ECM stiffness	Neurogenic markers (GDNF, BDNF, NGF, etc.) most up-regulated on 0.1–1 kPa hydrogels; myogenic markers (MYOG and Pax-7) most up-regulated on an 11 kPa hydrogel; and osteogenic markers (BMPs and BGLAP) most up-regulated on a 34 kPa hydrogel.[94]
	BM-MSCs	ECM stiffness	A 40 kPa hydrogel supported the highest level of (fourfold) VEGF expression; a 0.5 kPa hydrogel induced highest (25-fold) level of expression of EGF. All hydrogels had high (six- to ninefold) expression of HGF compared to a glass substrate.[133]
	BM-MSCs	ECM stiffness	A 30 kPa gel up-regulated fourfold expression of VEGF, up to twofold expression of IL-6, IL-7, IL-10, and bFGF compared to TCP. A 100 kPa gel down-regulated (twofold) expression of VEGF compared to TCP.[134]
	ADSCs	ECM stiffness	Compared to TCP, a 30 kPa substrate down-regulated expression of TGF-β1, Col I, and Col III by twofold; a 4 and a 13 kPa hydrogel down-regulated by 4–20-fold expression of TGF-β1, Col I, and Col III. Anti-HGF negated the antifibrotic activity of ADSC secretome.[135]
	BM-MSCs	ECM topography	A scaffold with 120 μm pore size up-regulated two- to threefold expression of HGF, bFGF, and LIF, as well as 150-fold expression of IGF, compared to TCP and scaffold with 5 nm pore size due to tenfold increase in expression of N-cadherin which mediates cell–cell interaction.[96]
	BM-MSCs	ECM topography	Substrate topography-induced elongated cell morphology with eccentric nuclei down-regulated 2.3- and 2.2-fold decrease in IL-6 and MCP-1 secretion, respectively; Spread-out cell morphology down-regulated expression of SDF-1 and HGF by up to fivefold compared to normal cell morphology.[95]

[a)] Abbreviations: BDNF (brain-derived neurotrophic factor), VEGF (vascular endothelial growth factor), NGF (nerve growth factor), IGF-1 (insulin-like growth factor-1), HGF (hepatocyte growth factor), FGF (fibroblast growth factor), SDF-1 (stromal cell-derived factor 1), Li-VPA (lithium and VPA cotreatment), NDNF (neuron-derived neurotrophic factor), BMP (bone morphogenetic protein), MMP (matrix metalloproteinase), DFO (deferoxamine), IFN-γ (interferon gamma), TNF-α (tumor necrosis factor alpha), TSG-6 (tumor necrosis factor-inducible gene 6), STC-1 (stanniocalcin-1), TGFb (transforming growth factor beta), GDNF (glial cell-derived neurotrophic factor), MYOG (myogenin), Pax (paired box protein), BGLAP (osteocalcin), EGF (epidermal growth factor), TCP (tissue culture polystyrene), LIF (leukemia inhibitory factor), MCP-1 (monocyte chemoattractant protein-1).

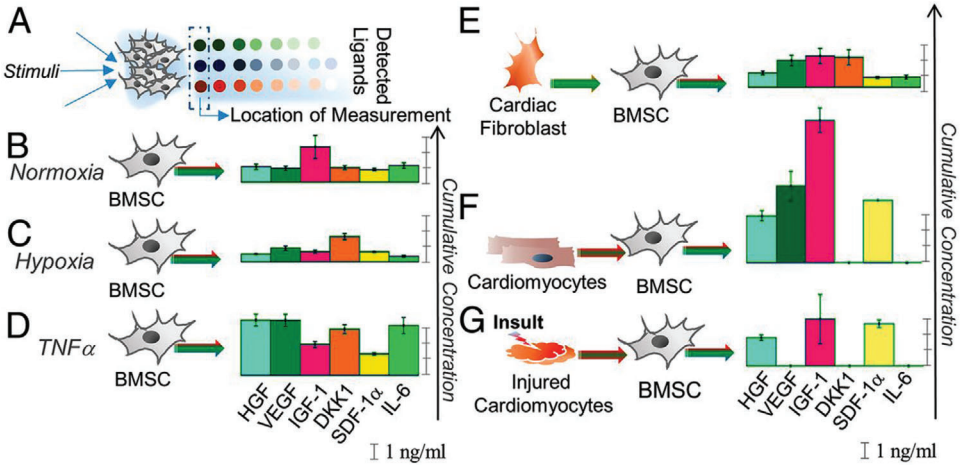

Figure 1. Secretion of BMSCs in response to specific environmental signals.[84] A) Secretion profiles were measured using detector microspots in an antibody array separated from the cell culture chamber by pillars at the 12 h time point. Cells displayed different secretory profiles in B) normoxic conditions, C) hypoxia condition, D) TNF-α stimulation, E) conditioned media from cardiac fibroblasts, F) conditioned media from human induced pluripotent stem cell-derived cardiomyocytes (hiPSC-CM), and G) conditioned media with hiPSC-CM insulted with peroxide to mimic ischemia reperfusion injury. Reproduced with permission.[84] Copyright 2019, National Academy of Sciences.

proteins.[81,82] The immunosuppressive function of MSCs can also be elicited through a variety of other chemokines, including tumor necrosis factor alpha (TNF-α), IL-1α, and IL-1β.[83,84]

4.3. Tuning Cell–Cell and Cell–ECM Interactions in MSC Culture

A growing body of evidence has suggested that cell–cell and cell-substrate interactions can modulate MSC activities and influence the MSC secretome.[85,86] Spheroid culture of MSCs is a commonly explored alternative to the 2D monolayer culture to condition MSC microenvironment. The 2D culture of MSCs often not only results in the loss of key cell receptors like those used in cell migration, but also significantly upregulates proinflammatory chemokines.[87] Spheroid culture on the other hand can better mimic the in vivo conditions by facilitating cell–cell and cell–ECM interactions, thus reducing apoptosis and enhancing angiogenic and anti-inflammatory components in the MSC secretome, including VEGF, PGE_2, FGF, IL-10, and BDNF, which has been linked to a greater level of neuronal differentiation.[87–90]

Another approach of preconditioning through the control of ECM microenvironment can be achieved by tuning matrix stiffness, topography, chemical composition, and geometry, all of which have been reported to modulate the MSC adhesion, proliferation, differentiation, migration, and organization.[91] MSCs are mechanosensitive, as shown in many studies regarding stem cell fate in response to mechanical stimulation.[92,93] Matrices that can induce high level of cell stress or otherwise capable of increasing contractility elevate the expression of genes linked to mechanotransduction and osteogenesis, whereas low stress-inducing substrates promote lower contractility and favor adipocytic cell fate.[94] The modulation of substrate topography had different effects on MSC cytokine secretion depending on cell type; and that cytokine secretion may be closely related to cell morphology.[95] For example, elongated MSC morphology was correlated with high levels of SDF-1 secretion while well spread-out MSC demonstrated up to fivefold lower SDF-1 secretion.[95] In another study on substrate structure, a macroporous scaffold with a mean pore size of ≈120 µm showed a higher secretion of VEGF, HGF, bFGF, IGF, and leukemia inhibitory factor (LIF) compared to a nanoporous hydrogel with a mean pore size of ≈5 nm. In a scratch wound healing assay, the macroporous scaffolds demonstrated significantly higher cell viability (80% vs 70%) and a higher degree of scratch closure after 20 h (75% vs 55%). These differences in secretion profile and in vivo results were attributed in part to the N-cadherin mediated cell–cell interactions between MSCs cultured in the macroporous scaffold, in contrast to the nanoporous scaffold which limited cell–cell interaction.[96]

In response to substrate stiffness, softer substrates (Young's modulus E ≈ 0.1–1 kilopascal, kPa) increased adipogenic differentiation of MSCs. As the substrate stiffness increased, myogenic differentiation (E ≈ 8–17 kPa) or osteogenic differentiation (E ≈ 25–40 kPa) predominantly occurred.[38,94] The osteogenic differentiation of MSCs was correlated with the increase in ligand density in addition to substrate stiffness, as revealed by the relationship between secretome and differentiation. The substrate stiffness caused an early change in the MSC secretome profile such as SDF-1, IGF-1, and thrombopoietin (TPO), which subsequently dictated the outcome of MSC differentiation (**Figure 2**).[38,91] The substrate properties such as stiffness, stress relaxation rate, and adhesion ligand density mediated MSC response and gene transcription as shown from the transcriptomic analysis; revealing a complex correlation between substrate stiffness and gene expression responding to differences in ligand-density and stress relaxation rate.[91] While the substrate stiffness drove the largest number of differentially expressed genes regardless of the other experimental parameters, these results as a whole demonstrated the complexity behind cell–ECM sensing interactions and the importance of contextualizing all ECM parameters when studying the effects of microenvironment on the MSC secretome.

Ample evidence has supported the notion that the secretome can be tailored to fit specific applications. Compared to hypoxia conditioning and treatment with bioactive agents, tuning

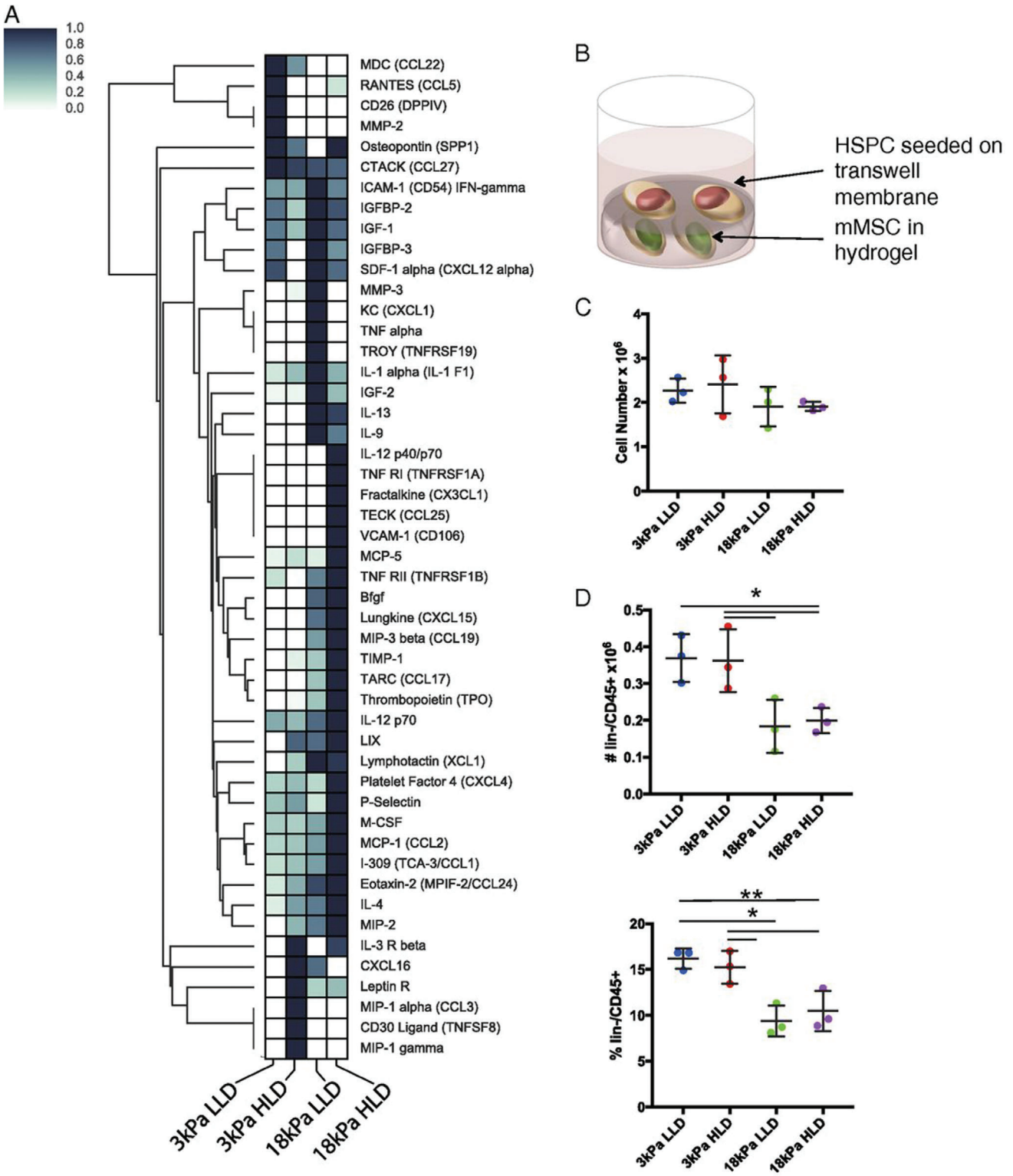

Figure 2. mMSCs-secreted cytokines in response to substrate stiffness.[91] A) Cytokine antibody array analysis was performed on conditioned media from mMSCs cultured in alginate hydrogels of varying stiffnesses and adhesion ligand (Arg-Gly-Asp) densities for 2–3 days, with values normalized to internal positive control and maximum signal for each material. B) Schematic of MSC and hematopoietic stem and progenitor cell (hSPC) coculture system. C) Viable cell number measured by flow cytometry after 1 week of coculture and D) number and percentage of $CD45^+/lin^-$ cells from transwell membrane measured by flow cytometry after 1 week of coculture. Reproduced with permission.[91] Copyright 2018, National Academy of Sciences.

cell–cell and cell–substrate interactions is an emerging approach, as the exact biophysical or biochemical mechanism that leads to changes in the secretome requires further elucidation. It has recently been shown that a combination of the listed secretome engineering methods may result in a synergistic effect. For example, the matrix stiffness of the alginate-based hydrogel regulated the level of TNF-α-induced gene expression from encapsulated MSCs:[86] MSCs in a softer matrix showed higher upregulation of immune response-related IL-6 and monocyte chemoattractant protein 1 (MCP-1/CCL2) compared to those in a stiff matrix, indicating a relationship between matrix stiffness and the effects of TNF-α treatment. Across the engineering techniques described here, it is important to emphasize that most reports that examine the MSC secretome are based on in vitro tests. There has been a growing effort to translate these findings to in vivo and clinical studies. However, due to the lack of reliable methods to measure secretome components in vivo, it has been challenging to profile the MSC secretome in response to changes in the MSC microenvironment. Moreover, the routes of secretome transport and subsequent paracrine signaling interactions still require clarification.

4.4. Crosstalk Between Macrophages and MSCs

MSCs have been documented to exhibit immunomodulatory functions in response to an inflammatory microenvironment.[97,98] In relation to monocytes and macrophages, MSCs have been shown to direct polarization toward an anti-inflammatory/immune regulatory phenotype. MSCs cocultured with $CD14^+$ monocytes of peripheral blood mononuclear cells (PBMCs) upregulated expression of IDO activity after IFN-γ exposure and induced the differentiation of the monocytes into IL-10-secreting M2-like macrophages, while suppressing lipopolysaccharide (LPS)-induced production of inflammatory cytokines (TNF-α, IL-1β, and IL-6) and indirectly suppressing T cell proliferation.[81,99] In another study, MSC-derived signaling factors in secreted EVs, particularly TGF-β1, pentraxin 3 (PTX3), and microRNA let-7b-5p and miR-21-5p, strongly correlated with immunosuppressive function in an autoimmune disease mice model; and the EVs effectively suppressed T cell receptor (TCR)-mediated or toll-like receptor 4 (TLR4)-stimulated splenocytes.[100] Generally speaking, secretome from early passage MSCs has a higher level of immunosuppression activity; and MSCs cultured in a 3D-matrix produce a higher level of EV components. A transwell coculture of macrophages with MSCs also showed reduced level of classically activated macrophage (M1) polarization, typically classified as proinflammatory, and an increased level of alternatively activated macrophage (M2) polarization, typically classified as proregenerative. MSC-derived EVs also induced M2 polarization, and infusion of MSCs without exosomes reduced M2 phenotype in macrophages, further linking the function of the MSC secretome in the crosstalk between MSCs and macrophages. Reciprocally, MSCs can also mediate macrophage recruitment and function through secretion of VEGF-A, PGE_2, nitric oxide (NO), and CCL2.[101] Through this crosstalk, MSCs promote the transition from monocyte to macrophage, and upregulate the expression of M2 marker CD206, while enhancing phagocytic capacity and shifting the metabolic status of inflammatory M1 macrophages to an M2-like phenotype.[102–104]

5. Delivery Strategies to Improve Therapeutic Effect of the MSC Secretome

MSCs exhibit promise in therapeutic efficacy in clinically translatable regenerative medicine applications due to their ability to differentiate into distinctive phenotypes and generate a regenerative microenvironment with paracrine signals, inhibit scar tissue formation, apoptosis, reduce inflammation, and promoting angiogenesis.[105] One of the major hurdles in successful clinical translation of cell-based therapy is limited cell survival, retention, and engraftment in the target tissue following injection or transplantation, which remains a critical requirement for effective treatment.[106] Various contributing factors include exposure of cells to ischemia and inflammation, emigration of transplanted cells from the injection site, and anoikis.[107] Previous studies have indicated that as low as 1% of MSCs survive 1 day after implantation in some treatment models.[108,109] While some studies continue to focus on improving MSC delivery and its effect on the target microenvironment,[110,111] the paradigm shift to paracrine signaling as the main therapeutic mechanism has led to many promising in vivo studies that utilize the MSC secretome itself, in the form of MSC-derived EVs, as a therapeutic method. Although EVs can bypass cellular challenges such as cell survival, the delivery of EVs remains a significant obstacle. The major approaches to delivery of MSC or MSC-derived EVs include direct injection, or injection with carriers such as tissue adhesives and hydrogels (**Table 3**). As characterization and potential modulation of the MSC secretome in vivo remain unclear, studies focusing on in vivo delivery of MSCs and EVs both aim to evaluate the effects on growth factors and cytokines within the target microenvironment.

5.1. Delivery of MSCs with Improved Adhesion Support

To overcome the issue of cell retention in direct injections of MSCs, one possible approach is to enhance cell-cell interactions and improve adhesion support through synthetic functionalized spheroids or MSC cell sheets. For example, MSC spheroids constructed by inducing cell–cell aggregation via supplement of a cell adhesion cue improved MSC survival and retention, and their therapeutic efficacy for treating ischemic diseases, as demonstrated by a 20- to 70-fold upregulation in angiogenic factors VEGF, PDGF, IGF, as well as 1250- to 1400-fold increase in epidermal growth factor (EGF) and angiopoietin-1(Ang-1) expression (**Figure 3**).[112] Through an alternative approach a hybrid MSC/PEGylated-DNA nanocomposite spheroid was generated for the treatment of glioblastoma. The MSCs were engineered to express TNF-related apoptosis-inducing ligand (TRAIL) while the PEGylated DNA facilitated colloidal stability upon calcium phosphate-mediated nanoprecipitation and allowed the loading of mitoxantrone, a drug that could sensitize the response of TRAIL in glioblastoma. Compared to single cell delivery, this hybrid MSC nanocomposite spheroid delivery improved MSC retention, resulting in up to 6.5-fold increase in SDF-1 receptor expression, and glioblastoma tropism of the transplanted MSCs in

Table 3. Major delivery methods for MSCs and MSC-derived EVs.

Delivery method [a]	Components involved	Treatment model	Key outcomes
Encapsulation and sustained release, e.g., hydrogels or microparticles	BM-MSCs spheroid delivered in collagen-pullulan gel	Stented excisional wound mouse model, local implant to wound site	Eight- to tenfold increase of VEGF and MCP-1 secretion in hydrogel culture compared to 2D culture. 15–30% faster complete wound healing time compared to local injection of MSCs, unseeded scaffold, and no treatment.[117]
	BM-MSCs delivered in microgel prepared from type-I atelocollagen, 4S-StarPEG	Hindlimb ischemia mouse model, local implant to proximal artery	Upregulated three- to sevenfold expression of Ang-1, bFGF, and VEGF-A compared to cells or microgel alone. Demonstrated at least 25% increase in blood vessel density.[128]
	BM-MSC spheroids delivered with PEG-DNA, Ca^{2+} microparticles	Subcutaneous tumor mouse model, local injection into tumor site	Upregulated 2–6.5-fold expression of CXCR-4 (receptor specific for SDF-1) and similarly demonstrated 1.5–2-fold increase in migration speed and distance. MSC expression of TNF-related apoptosis-inducing ligand resulted in 85% reduction of glioblastoma tumor size compared to PBS control.[109]
Delivery of MSCs with improved adhesion support, e.g., spheroids or cell sheets	8-PEG-RGD-modified ADSC spheroids	Hindlimb ischemia mouse model, intramuscular injection	Upregulated 20-fold expression of VEGF, 50–70-fold of PDGF and IGF, and upregulated 1250–1400-fold expression of EGF and Ang-1 compared to 2D culture. Similar levels of apoptosis, fibrosis, and inflammation compared to untreated control, 6–15-fold downregulation compared to PBS.[108]
	ADSC cell sheet	Myocardial infarction rat model, transplant onto scar site	Upregulated five- to tenfold expression of VEGF and HGF; improved cardiac function in a heart failure model; threefold improvement in left ventricular end diastolic pressure and plasma atrial natriuretic peptide compared to the untreated control.[110]
	Umbilical-derived MSC cell sheet	Subcutaneous dorsal incision mouse model, subcutaneous transplant onto incision site	HGF continuously secreted for at least 10 days after subcutaneous implantation; improved vascularization compared to the negative control without cell sheet treatment; reduced TNF-α secretion to healthy background level.[129]
Delivery of MSC-derived EVs	ES-MSC-derived EVs	Chronic liver injury rat model, intraperitoneal injection	Downregulated two- to fourfold expression of TIMP-1 and TNF-α, upregulated 2- and 40-fold expression of anti-inflammatory cytokine IL-10 and MMP13, respectively, compared to PBS control.[130]
	BM-MSC-derived EVs	Dry eye mouse model, direct injection into intraorbital lacrimal gland	Early-passage (15 population doublings) EVs downregulated two- to threefold expression of TNF-α and proinflammatory cytokines IL-1β and IL-6 compared to PBS and late-passage (40 population doublings) EVs.[98]
	BM-MSC-derived EVs	Traumatic brain injury mouse model, intravenous injection	Downregulated up to twofold expression of proinflammatory cytokine IL-1β at 12 h after injection of BM-MSC-derived EVs given at 1 h post traumatic brain injury, in comparison with PBS injection or i.v. delivery of MSCs alone.[111]
	ADSC-derived EVs delivered in pDA-coated PLGA scaffold	Calvarial skull defect mouse model, local implant to defect site	Threefold increase in bone regeneration compared to the pDA-coated PLGA scaffold alone. Upregulated 1.5–2-fold expression of ALP and RUNX2 relative to control osteogenic growth media over 14 days.[123]
	BM-MSC-derived EVs delivered in Hystem hydrogel	Calvarial skull defect rat model, local implant to defect site	Over twofold increase in bone volume formation compared to the hydrogel alone. Upregulated two- to fourfold expression of ALP, OCN, OPN, and RUNX2 compared to the negative control group containing no miRNAs after 3 days post-treatment.[124]
	Placenta-MSC-derived EVs delivered in chitosan hydrogel	Hindlimb ischemia mouse model, intramuscular injection	1.5-fold increase in capillary formation and over fivefold reduction in collagen formation at the wound site compared to PBS treatment after 14 days postinjection. 2.5-fold reduction in ambulatory impairment in functional tests.[125]

[a] Abbreviations: VEGF (vascular endothelial growth factor), MCP-1 (monocyte chemoattractant protein-1), PEG (polyethylene glycol), Ang-1 (angiopoietin-1), bFGF (basic fibroblast growth factor), SDF-1 (stromal cell-derived factor 1), CXCR (C-X-C motif chemokine receptor), TNF (tumor necrosis factor), PBS (phosphate-buffered saline), PDGF (platelet-derived growth factor), IGF (insulin-like growth factor), EGF (epidermal growth factor), HGF (hepatocyte growth factor), TIMP-1 (tissue inhibitor of metalloproteinase-1), ALP (alkaline phosphatase), ES-MSC (embryonic stem cell-derived MSCs), pDA (polydopamine), PLGA (poly(lactic-*co*-glycolic acid)), RUNX2 (runt-related transcript factor-2), OCN (osteocalcin), OPN (osteopontin).

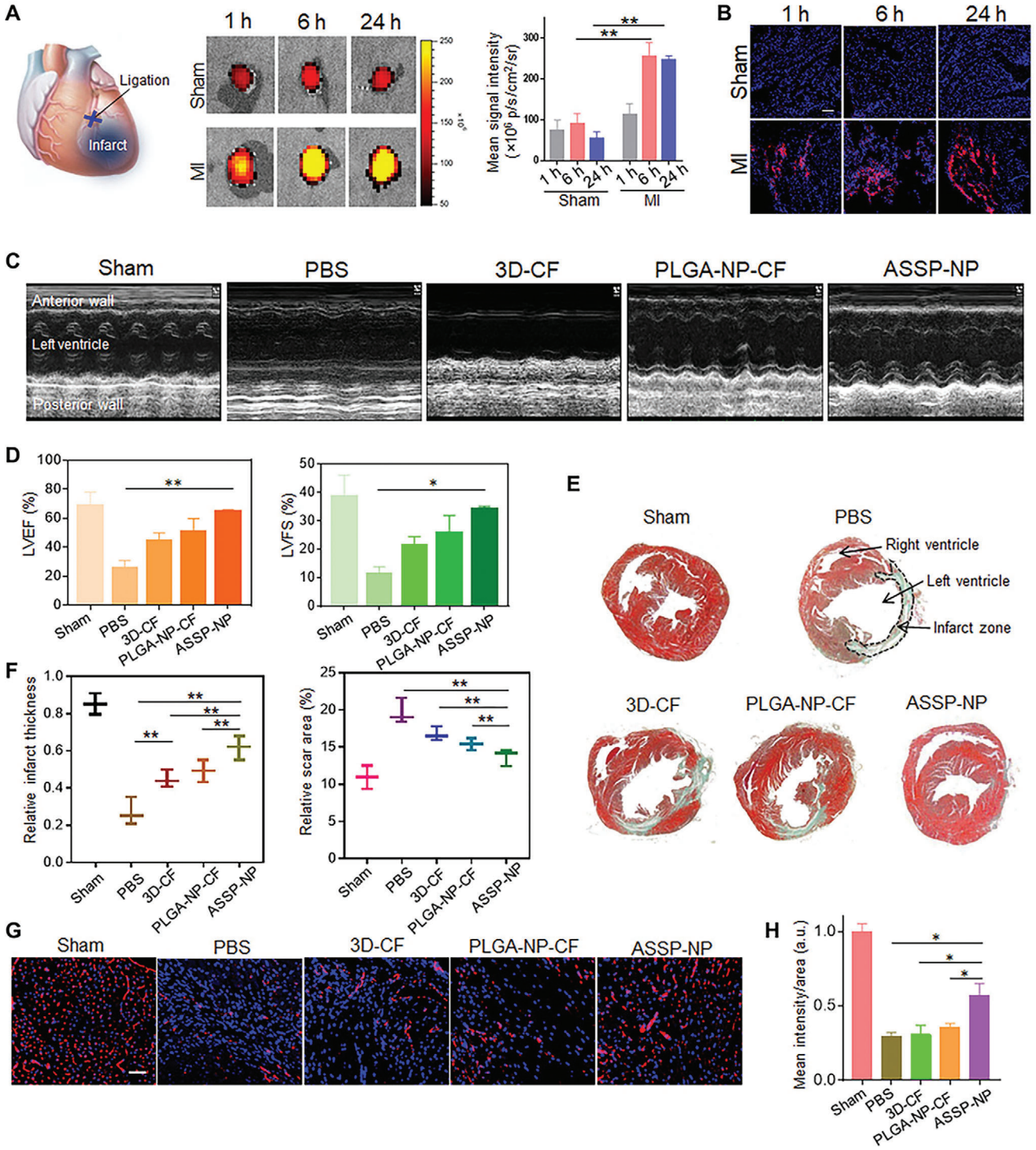

Figure 3. Intravenous administration of artificial stem cell spheroid nanoparticles (ASSP-NP) in a mouse MI model for cardiac repair.[112] A) Ex vivo fluorescent imaging of mouse hearts and quantitative analysis of fluorescence intensities at different time points after tail vein injection of ASSP-NPs in sham and MI mice. B) ASSP-NP distribution in sham (nonischemic) and MI (ischemic) cardiac tissue at different time points following intravenous injection. C) Echocardiography images of left ventricular wall motion with or without treatments following MI surgery at 28 days using PBS, cocktail factor containing conditioned media from 3D SSP (3D-CF), PLGA nanoparticles (PLGA-NP-CF), and targeted ASSP nanoparticles (ASSP-NP) with red blood cell membrane and platelet membrane coatings. D) Quantification of echocardiography functional assay, including left ventricular ejection fraction (LVEF) percentage and left ventricular fractional shortening (LVFS) percentage. E) Masson's trichrome staining of midpapillary sections of the heart at 28 days after MI. F) Quantitative analysis of infarct wall thickness and scar area. G) Representative images and H) image-based quantification of blood vessels in cardiac ischemic conditions by anti-CD31 antibody immunostaining at 28 days after treatments. Reproduced with permission.[112] Copyright 2020, American Association for the Advancement of Science.

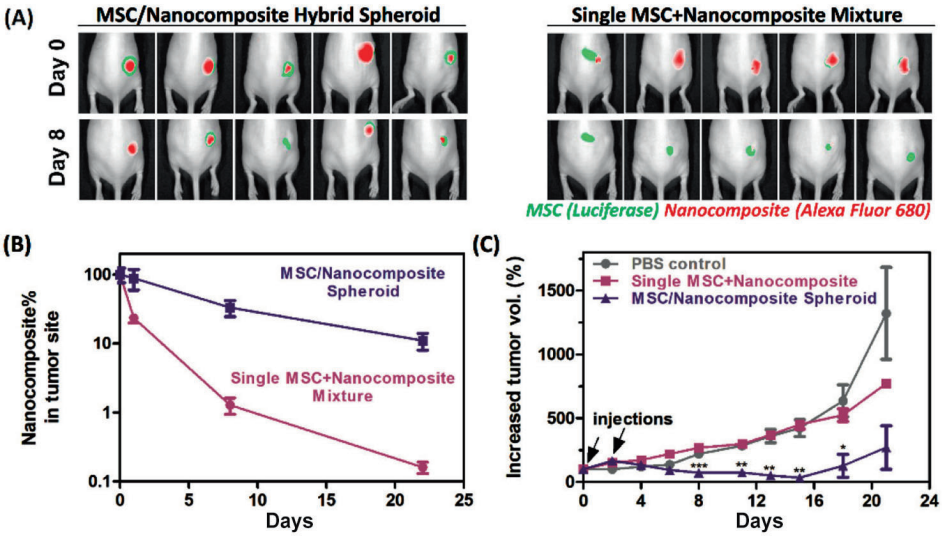

Figure 4. MSC/nanocomposite spheroid improves tumor homing of MSCs and reduction tumor volume growth.[113] A) Mice treated with hybrid spheroids generated with a microfluidics-based approach and PEGylated DNA template or single MSC-nanocomposite mixture through injection at the boundary of the tumor site on days 0 and 2, and quantification B,C) of tumor homing and inhibition. Reproduced with permission.[113] Copyright 2019, American Chemical Society.

a U87 xenograft mouse model (**Figure 4**). These effects in the MSC spheroids were attributed to a boost in C-X-C chemokine receptor type 4 (CXCR4) on MSCs, which are involved in sensing chemotaxis.[113]

Another approach to enhancing cell–cell interactions and adhesion support involves maximizing cell–cell contact to address issues in engraftment and retention. The ECM sheet secreted by an ADSC monolayer has been shown to facilitate cell-target tissue adhesion in a myocardial infarction rat model.[114] The transplantation of an ADSC sheet improved functional recovery as shown from the decreasing left ventricle end-diastolic pressure and plasma atrial natriuretic peptide by around 70%; both parameters of which are normally drastically increased during myocardial infarction. The ADSC sheet also showed significantly increased secretion of angiogenic factors with five- to tenfold higher expression of VEGF and HGF than the other experimental groups.

5.2. Delivery of MSC-Derived EVs

The approach of injecting EVs not only presents an attractive alternative that entirely avoids the issues of cell survival, retention, and engraftment, but also distinguishes the direct therapeutic benefits of the MSC secretome for in vivo models. BM-MSC-derived EVs have been applied to suppress neuroinflammation in a traumatic brain injury mice model (**Figure 5**).[115] This approach not only resulted in a decrease in astrocytic scarring and twofold downregulation of proinflammatory cytokine IL-1β in the brain, but also significant functional recovery a month after the initial injury. In an object-based behavioral test, only the EV-treated group was able to retain the ability of pattern separation, which can be described as the ability to store similar but nonoverlapping memories and recognize novel objects. Similarly, in a water maze test, preservation of the spatial learning ability was only observed in the EV-treated group. The immunomodulatory effects of BM-MSC-derived EVs were also studied through direct injection into the intraorbital lacrimal gland in an ocular Sjögren's syndrome (dry eye) mouse model.[100] At the 1week timepoint, the ocular surface and intraorbital gland exhibited two- to fourfold lower expression of proinflammatory growth factors and cytokines TNF-α, IL-1β, and IFN-γ in the EV treatment group compared to the phosphate-buffered saline (PBS) control group. It is worth noting that the therapeutic efficacy of BM-MSC-derived EVs was dependent on the passage number of the cells. The early passage BM-MSC-derived EVs (< 15 population doubling) demonstrated immunomodulatory potential, whereas the late passage BM-MSC-derived EVs (> 40 population doubling) no longer showed immunomodulatory effects compared to the PBS control group. Identification of the optimal preparation of EVs clearly requires further examination, along with elucidating appropriate dosing levels and the specific mechanism behind EV transport.

5.3. Biomaterials for MSC Delivery

Approaches to increase survival rate of the transplanted MSCs have been explored to improve the effectiveness of cell-based therapies, which include modulating cell metabolism by altering the repair environment with biomaterials in order to promote cell adaptation to a harsh implantation environment.[116] Hydrogel scaffolds for cell encapsulation can serve to regulate MSC metabolic activities and facilitate cellular functionalization. Oxygen tension levels, glucose supply, mechanical stress, and pH level can regulate metabolic pathways of MSCs and energy consumption rate, thus influencing cell survival and their therapeutic efficacy.[116,117] For example, MSCs encapsulated in a graphene oxide (GO)/alginate composite microgel through electrospraying were used to improve cell viability in the infrared environment in the cardiac tissue. MSCs cocultured with cardiomyocytes in a

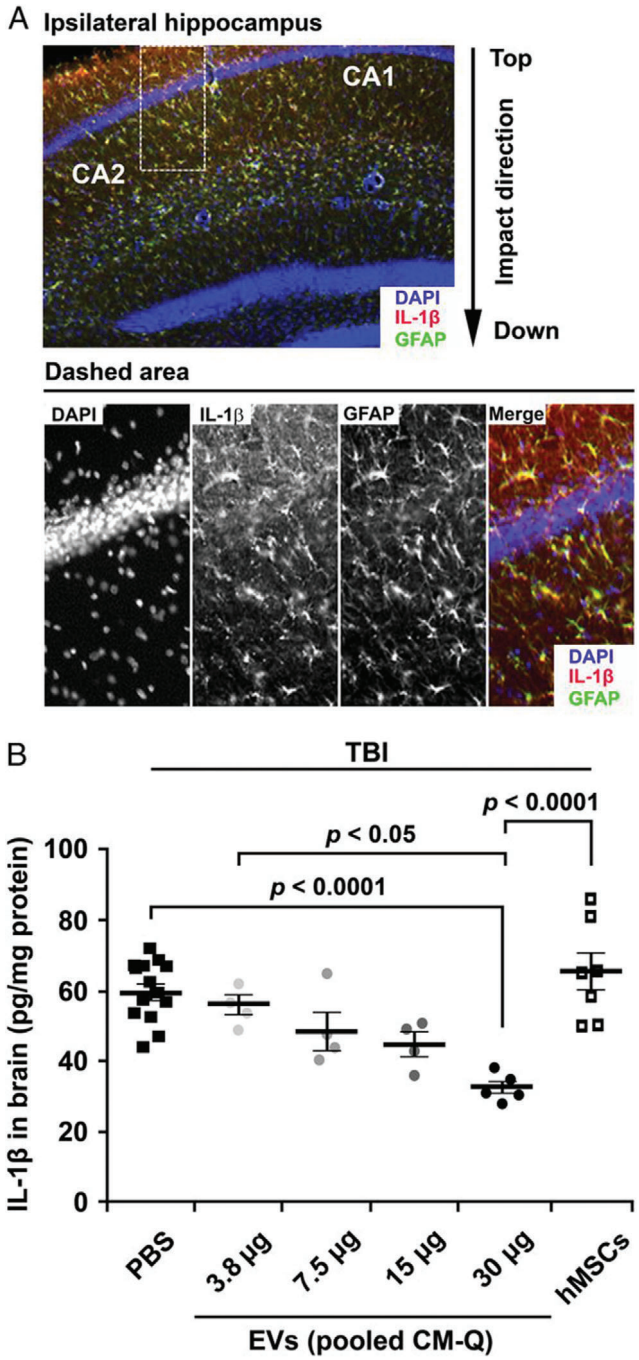

Figure 5. EV Dose-response data for suppression of neuroinflammation after traumatic brain injury (TBI).[115] A) Immunohistochemistry staining of brain sections after TBI mouse model. B) Decreased levels of IL-1β in a dose-dependent manner of PBS or EVs administrated 1 h after TBI measured by ELISA on homogenates from ipsilateral brain sections isolated 12 h after TBI. Reproduced with permission.[115] Copyright 2015, National Academy of Sciences.

composite hydrogel matrix increased cytokine production compared to a 2D coculture by two- to fivefold, and further reduced scarring and greater left ventricular thickness.[118]

Cell-supporting scaffolds can provide suitable ECM microenvironment to anchor the delivered cells. An ideal ECM to support cells is a 3D network composed of fibrous matrix, which provides structural integrity for cellular anchorage and naturally sequesters soluble signals.[119] Typically, such a scaffold should also mimic the ECM structure of the target tissue. A wide range of natural biomaterials-derived hydrogels, such as collagen, fibrin, chitosan, dextran, hyaluronic acid, alginate, and Matrigel, have been tested for MSC delivery due to their high degrees of biocompatibility and bioactivity.[119] To overcome low cell retention, fibrin gel was used to entrap MSC spheroids.[107] When cultured in serum-free media and hypoxic conditions (1% oxygen), MSCs delivered in fibrin reduced apoptotic activity and increased up to 100-fold levels of VEGF secretion compared to injection of a single cell suspension, while maintaining their osteogenic potential in the repair of bone defects.[120] The codelivery of MSCs with anti-miR199a has also been studied in vivo to improve MSC secretion profile through the upregulation of HIF-1α. Rabbit bone marrow MSCs and anti-miR199a codelivered by nanofibrous spongy microspheres enhanced MSC seeding, proliferation, and differentiation, and facilitated regeneration of the nucleus pulposus tissue.[121] With sustained in situ release of anti-miR-199a, this delivery approach enhanced HIF-1α and SOX-9 activities of the MSCs to reduce mineralization, leading to the suppression of calcification and promotion of nucleus pulposus formation.

A pullulan-collagen based hydrogel was also tested for improving the delivery efficiency of MSCs in a stented excisional cutaneous wound healing model. The hydrogel was shown as an effective matrix to support MSCs as a powerful effector in secreting angiogenic and chemo-attractive factors, VEGF and MCP-1, to support angiogenic activity.[122] The increased secretome activity was mirrored by significantly accelerated healing in wounds treated with MSC-encapsulated hydrogels. Although no significant differences could be observed between the local MSC treatment group and the no treatment group, animals received the MSC-encapsulated hydrogel healed the wound nearly 2 days faster with a threefold increase in vascularization compared to the no treatment group. A further assessment of MSC viability and engraftment suggested that the hydrogel not only enhanced MSC survival, but also promoted MSC proliferation.[122]

5.4. Biomaterials for Delivery of MSC-Derived EVs

As a cell-free alternative, biomaterials-based delivery of EVs circumvents several important challenges associated with managing cell survival and metabolism. However, EV delivery also needs to address the issue of rapid diffusion and clearance from the tissue repair site. The stability of EVs as well as the stability of their contents, particularly growth factors and miRNAs, under physiological conditions throughout the delivery duration need to be maintained. Various biomaterials have been designed and optimized to improve the delivery efficiency of MSC-derived EVs by offering advantages over an extended release duration, protection against degradation, and enhancing the therapeutic capacity of the EVs.

The use of biomaterials for EV delivery has been explored in bone regeneration to facilitate osteoblastic differentiation. In a murine calvarial bone defect model, the osteogenic potential of the ADSC-derived EVs was demonstrated through delivery with a polydopamine-coated poly(lactic-*co*-glycolic acid) (PLGA/pDA) scaffold.[123] The polydopamine coating facilitated immobilization of bone forming peptide 1 (BFP-1) as well as the engraftment of exosomes, resulting in a slow-release profile of these two components over 8 days rather than the typical burst release and complete depletion by day 4. Enhanced bone regeneration was observed in the group received PLGA/pDA containing exosomes, which was primarily attributed to a twofold increase in host MSC recruitment in the presence of exosomes. In a rat calvarial bone defect model, BM-MSC-derived EVs delivered using a Hystem-HP hydrogel scaffold rich in collagen and hyaluronic acid showed strong osteogenic outcomes in vivo.[124] The hydrogel-delivered EVs resulted in over a threefold increase in bone formation relative to the hydrogel only group. In vitro functional characterization of the EVs revealed that the increased osteogenic expression was mainly facilitated through miRNA cargo including miR-196a, miR-27a, and miR-206.

A thermosensitive chitosan hydrogel was evaluated for delivery of EVs secreted by human placenta-derived MSCs due to its in situ setting property and good biocompatibility.[125] The level of a key paracrine signaling molecule miR-126 was maintained at 50% from the EVs loaded in the chitosan hydrogel, in contrast to the complete depletion in the control group with EVs only. The retention studies in a murine hindlimb ischemia model showed a similar trend, where the incorporation of the chitosan hydrogel significantly improved the retention of EVs at the site of injection, resulting in an increased endothelium-protective capacity of the EVs delivered in the hydrogel and a fivefold reduction in fibrosis within the wounded tissue. In addition, the antifibrotic and angiogenic responses of EVs delivered by the hydrogel were stronger than the EV injection alone, even though the hydrogel alone showing no significant therapeutic benefit. These results suggest that the hydrogel delivery effectively improve the therapeutic outcomes of MSC-derived EVs due to improved retention and stability.

6. Conclusion

Due to the challenges associated with cell retention and survival in MSC delivery, the use of MSC-derived EVs or conditioned media for the purpose of delivering paracrine signals including miRNAs and growth factors, has garnered increasing interest building from the favorable outcomes obtained from the early phase studies discussed above. For MSC secretome delivery, concentrated EVs or specific signaling molecules can be collected, lyophilized, and stored until use without the need for cell expansion culture or sophisticated storage and handling protocols. During the production of EVs, it is possible to apply the approaches listed in Table 1 to tailor the compositions of EVs with optimized bioactivity tailored for tissue-specific applications, since cell culture conditions can be readily controlled in an in vitro context. The delivery dose or concentration of the EVs can also be controlled with a higher degree of versatility than that of MSCs, as EVs can be isolated and concentrated more easily than MSCs. The major challenge for EV application is the added layer of batch-to-batch variation between productions. To partially address this, it is possible to develop a specific set of paracrine cues, based on learnings from the secretome studies, which can be used as a well-defined formulation. It is important to note that, as studies elucidate the mechanisms behind repair influenced by paracrine signaling cues, the relative ratios or balance of EV components may play an important role in determining repair outcomes that purified cytokine or growth factor delivery fails to accurately capture. As an alternative, MSC delivery with an optimized system offers a dynamic system to promote tissue repair, where MSCs responding to microenvironmental cues may secrete a specific set of proregenerative secretome. Moreover, for patients with reduced regenerative capacity (e.g., ageing, trauma, immunosuppression), the ability for native MSCs to respond effectively may hamper the regenerative response. Therefore, a healthy supply of proangiogenic and anti-inflammatory cells could better serve these applications. In contrast, EV delivery has the limit of a static population of EVs predetermined at the time of injection. Nevertheless, EVs and other direct applications of the MSC secretome are promising alternatives to MSC therapy; and have been or are currently tested in a handful of clinical trials initiated over the past few years (**Table 4**). Most of these trials remain in the early phases or with undisclosed results, but they show the potential clinical translatability in various applications such as treatments of osteoarthritis, ischemic stroke, and coronavirus-related diseases. Along with overcoming the previously mentioned challenges in batch-to-batch variation and optimization of treatment dosage, advances in effective scaffolds or carriers to deliver EVs at the tissue repair site in a spatially and temporally controlled fashion will be critical to realize the full therapeutic benefits of MSC-derived EVs.[26,126]

As the field advances toward clinical success through the immunomodulatory and regenerative potential of MSCs, there is an increasing need to understand the paracrine signaling effects from MSC therapies. The importance of the secretome has led to growing efforts to engineer its expression through MSC preconditioning, such as using bioactive agents or tuning the ECM microenvironment, and to develop delivery vehicles that modulate paracrine signal release. Therefore, the use of biomaterials to improve localization and survival of MSCs can be combined with the strategies to expand their capacity in promoting tissue regeneration or repair. Moreover, gene editing in MSCs or direct loading of miRNA or anti-miRNA to EVs allow for more precise tuning of MSC therapeutic activity and secretome profile for tailored applications. The myriad of biomaterials composition, dynamic tuning of mechanical property, tailoring MSC source, organization, and preconditioning, and optimizing delivery approaches offers a highly tunable and modular approach to MSC regenerative therapeutics (**Figure 6**). On the mechanistic side, the combination of these approaches has led to a focus on tuning the immunomodulatory response, as well as angiogenesis and host tissue ingrowth, opening up exciting opportunities for MSC-based regenerative therapy. Across different tissue and organ systems, the biomaterials-based scaffolds mimicking the ECM microenvironmental cues can influence MSC fate in vivo, altering, not only EV release or paracrine signaling, but also the subsequent secretion of extracellular matrix components and tissue organization to stabilize or repair the target tissue. A better understanding of each of these factors will serve to improve

Table 4. Ongoing clinical trials utilizing the MSC secretome.

Clinical indication[a)]	Mode of therapeutic action	Added modifications	Year started	Phase	Status	Trial number
Osteoarthritis	Umbilical-derived MSC conditioned medium	Unmodified	2020	1/2	Recruiting	NCT04314661
Chronic ulcer wound	WJ-MSC conditioned medium	Modified to form a topical gel, unclear how	2019	1	Completed	NCT04134676
Novel coronavirus pneumonia	ADSC-derived exosomes	Unmodified	2020	1	Completed	NCT04276987
Ischemic stroke	MSC-derived exosomes, unspecified source	Enriched by miR-124	2017	1/2	Recruiting	NCT03384433
Periodontitis	ADSC-derived exosomes	Unmodified	2020	1	Recruiting	NCT04270006
Macular holes	Umbilical-MSC-derived exosomes	Unmodified	2018	1	Recruiting	NCT03437759
Dystrophic epidermolysis bullosa	BM-MSC-derived exosomes	Unspecified, AGLE-102 product	2019	1/2A	Not yet recruiting	NCT04173650
Neonatal bronchopulmonary dysplasia	BM-MSC-derived exosomes	Unspecified, UNEX-42 product	2019	1	Recruiting	NCT03857841

[a)] Abbreviations: MSC (mesenchymal stem cell), WJ (Wharton's Jelly), ADSC (adipose tissue-derived stem cell), BM (bone marrow).

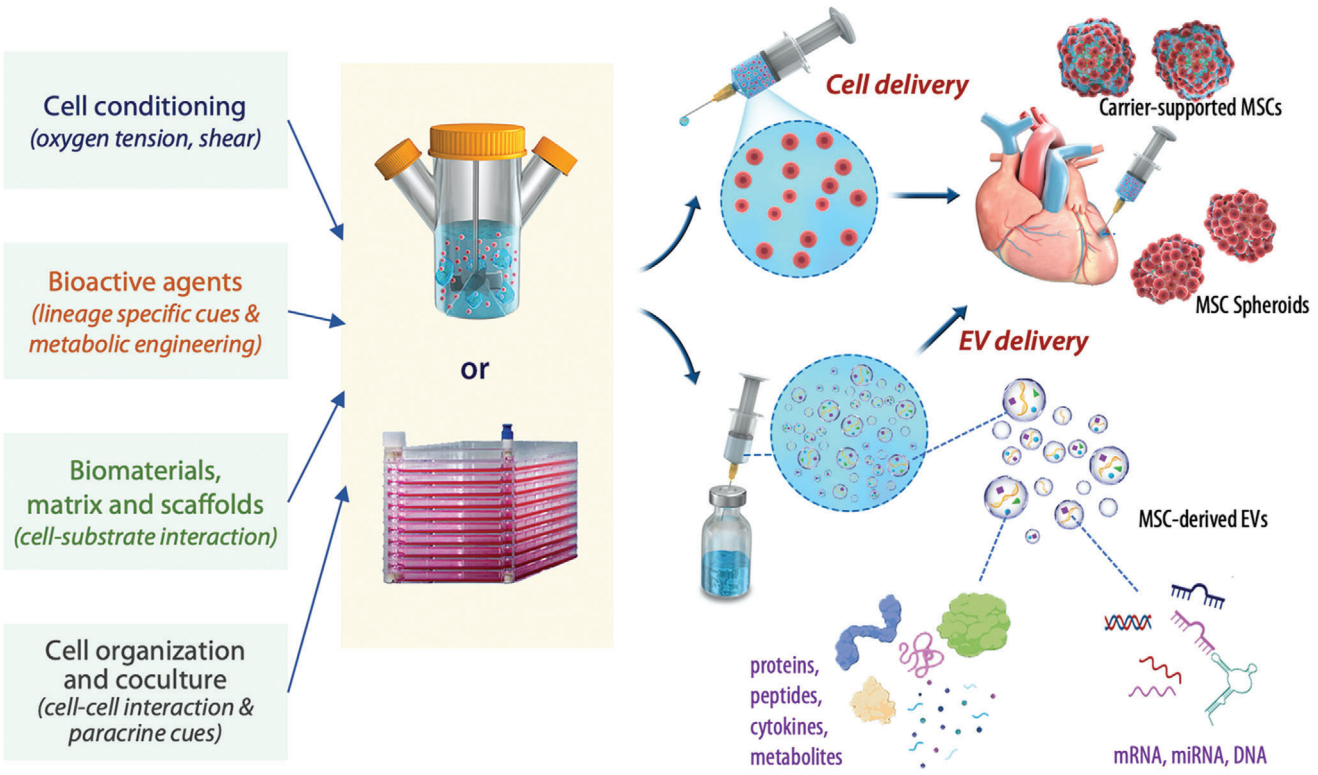

Figure 6. Tuning of the MSC secretome profile for the delivery of engineered MSCs and paracrine cues. MSC secretome can be modulated by adjusting cell culture conditions, supplementing bioactive agents, employing biomaterials matrix or scaffold, and modulating cell–cell interactions. These engineering approaches can be adopted to adjust the quantities and components of MSC paracrine signals prior to cell delivery to the treatment site. For cell delivery, the engineered MSCs can be injected in the form of MSC spheroids or carrier-supported MSCs, or biomaterials delivered with the MSCs. The secretome can also be delivered in the form of EVs enriched from the cultured MSCs prior to delivery. The EVs contain proteins, peptides, cytokines, metabolites, as well as nucleic acids including mRNA, miRNA, and DNA.

clinical outcomes and inform standardized practices for MSC-based therapies.

Acknowledgements

C.C. and J.Y. contributed equally to this work. This work was partially supported by the National Institute of Neurological Diseases and Stroke (No. R21NS096668) and the Helmsley Foundation.

Conflict of Interest

The authors declare no conflict of interest.

Keywords

biomaterials, extracellular vesicles, mesenchymal stem cells, microRNA, paracrine signaling, secretome

Received: September 22, 2020
Revised: December 13, 2020
Published online: January 12, 2021

[1] A. I. Caplan, *J. Orthop. Res.* **1991**, *9*, 641.
[2] M. Dominici, K. Le Blanc, I. Mueller, I. Slaper-Cortenbach, F. C. Marini, D. S. Krause, R. J. Deans, A. Keating, D. J. Prockop, E. M. Horwitz, *Cytotherapy* **2006**, *8*, 315.
[3] P. A. Zuk, M. I. N. Zhu, H. Mizuno, J. Huang, J. W. Futrell, A. J. Katz, P. Benhaim, H. P. Lorenz, M. H. Hedrick, *Tissue Eng.* **2001**, *7*, 211.
[4] N. D. C. Noronha Nc, A. Mizukami, C. Caliári-Oliveira, J. G. Cominal, J. L. M. Rocha, D. T. Covas, K. Swiech, K. C. R. Malmegrim, *Stem Cell Res. Ther.* **2019**, *10*, 131.
[5] S. Shi, S. Gronthos, *J. Bone Miner. Res.* **2003**, *18*, 696.
[6] C. De Bari, F. Dell'Accio, P. Tylzanowski, F. P. Luyten, *Arthritis Rheum.* **2001**, *44*, 1928.
[7] P. Robey, *F1000Research* **2017**, *6*, 524.
[8] S. Viswanathan, Y. Shi, J. Galipeau, M. Krampera, K. Leblanc, I. Martin, J. Nolta, D. G. Phinney, L. Sensebe, *Cytotherapy* **2019**, *21*, 1019.
[9] Y. Muguruma, T. Yahata, H. Miyatake, K. Ando, T. Hotta, *Blood* **2004**, *104*, 1283.
[10] F. E. Ezquer, M. E. Ezquer, J. M. Vicencio, S. D. Calligaris, *Cell Adhes. Migr.* **2017**, *11*, 110.
[11] A. Y. Clark, K. E. Martin, J. R. García, C. T. Johnson, H. S. Theriault, W. M. Han, D. W. Zhou, E. A. Botchwey, A. J. García, *Nat. Commun.* **2020**, *11*, 114.
[12] C. Loebel, R. L. Mauck, J. A. Burdick, *Nat. Mater.* **2019**, *18*, 883.
[13] A. R. Williams, B. Trachtenberg, D. L. Velazquez, I. McNiece, P. Altman, D. Rouy, A. M. Mendizabal, P. M. Pattany, G. A. Lopera, J. Fishman, *Circ. Res.* **2011**, *108*, 792.
[14] P. J. Psaltis, A. C. W. Zannettino, S. G. Worthley, S. Gronthos, *Stem Cells* **2008**, *26*, 2201.
[15] C. T. J. van Velthoven, A. Kavelaars, F. van Bel, C. J. Heijnen, *Brain Res. Rev.* **2009**, *61*, 1.
[16] V. Sueblinvong, D. J. Weiss, *Curr. Opin. Pharmacol.* **2009**, *9*, 268.
[17] Q. Zhao, H. Ren, D. Zhu, Z. Han, *Biol. Cell* **2009**, *101*, 557.
[18] B. Bussolati, P. V. Hauser, R. Carvalhosa, G. Camussi, *Curr. Stem Cell Res. Ther.* **2009**, *4*, 2.
[19] J. Y. Oh, M. K. Kim, M. S. Shin, H. J. Lee, J. H. Ko, W. R. Wee, J. H. Lee, *Stem Cells* **2008**, *26*, 1047.
[20] K. Lau, R. Paus, S. Tiede, P. Day, A. Bayat, *Exp. Dermatol.* **2009**, *18*, 921.
[21] R. Passier, L. W. van Laake, C. L. Mummery, *Nature* **2008**, *453*, 322.
[22] K. C. Wollert, H. Drexler, *Nat. Rev. Cardiol.* **2010**, *7*, 204.
[23] S. F. A. Askar, A. A. Ramkisoensing, D. E. Atsma, M. J. Schalij, A. A. F. de Vries, D. A. Pijnappels, *Circ.: Arrhythmia Electrophysiol.* **2013**, *6*, 380.
[24] D. García-Sánchez, D. Fernández, J. C. Rodríguez-Rey, F. M. Pérez-Campo, *World J. Stem Cells* **2019**, *11*, 748.
[25] N. Haque, N. H. A. Kasim, M. T. Rahman, *Int. J. Biol. Sci.* **2015**, *11*, 324.
[26] M. Mendt, K. Rezvani, E. Shpall, *Bone Marrow Transplant.* **2019**, *54*, 789.
[27] M. F. Pittenger, D. E. Discher, B. M. Péault, D. G. Phinney, J. M. Hare, A. I. Caplan, *npj Regen. Med.* **2019**, *4*, 22.
[28] J. Q. Yin, J. Zhu, J. A. Ankrum, *Nat. Biomed. Eng.* **2019**, *3*, 90.
[29] S. H. Ranganath, O. Levy, M. S. Inamdar, J. M. Karp, *Cell Stem Cell* **2012**, *10*, 244.
[30] K. Iwasaki, A. R. Ahmadi, L. Qi, M. Chen, W. Wang, K. Katsumata, A. Tsuchida, J. Burdick, A. M. Cameron, Z. Sun, *Sci. Rep.* **2019**, *9*, 7149.
[31] G. Lou, Z. Chen, M. Zheng, Y. Liu, *Exp. Mol. Med.* **2017**, *49*, e346.
[32] D. Z. Sun, B. Abelson, P. Babbar, M. S. Damaser, *Nat. Rev. Urol.* **2019**, *16*, 363.
[33] K. J. Brown, C. A. Formolo, H. Seol, R. L. Marathi, S. Duguez, E. An, D. Pillai, J. Nazarian, B. R. Rood, Y. Hathout, *Expert Rev. Proteomics* **2012**, *9*, 337.
[34] D. Kehl, M. Generali, A. Mallone, M. Heller, A.-C. Uldry, P. Cheng, B. Gantenbein, S. P. Hoerstrup, B. Weber, *npj Regen. Med.* **2019**, *4*, 8.
[35] L. Bundgaard, A. Stensballe, K. J. Elbæk, L. C. Berg, *Stem Cell Res. Ther.* **2020**, *11*, 187.
[36] S.-J. J. Park, R. Y. Kim, B.-W. W. Park, S. Lee, S. W. Choi, J.-H. H. Park, J. J. Choi, S.-W. W. Kim, J. Jang, D.-W. W. Cho, H.-M. Chung, S.-W. Moon, K. Ban, H.-J. Park, *Nat. Commun.* **2019**, *10*, 3123.
[37] B.-W. Park, S.-H. Jung, S. Das, S. M. Lee, J.-H. Park, H. Kim, J.-W. Hwang, S. Lee, H.-J. Kim, H.-Y. Kim, S. Jung, D.-W. Choo, J. Jang, K. Ban, H.-J. Park, *Sci. Adv.* **2020**, *6*, eaay6994.
[38] Y. Martín-Martín, L. Fernández-García, M. H. Sanchez-Rebato, N. Marí-Buyé, F. J. Rojo, J. Pérez-Rigueiro, M. Ramos, G. V. Guinea, F. Panetsos, D. González-Nieto, *Sci. Rep.* **2019**, *9*, 8801.
[39] S. W. Ferguson, J. Wang, C. J. Lee, M. Liu, S. Neelamegham, J. M. Canty, J. Nguyen, *Sci. Rep.* **2018**, *8*, 1419.
[40] Q. Xue, C. Yu, Y. Wang, L. Liu, K. Zhang, C. Fang, F. Liu, G. Bian, B. Song, A. Yang, G. Ju, J. Wang, *Sci. Rep.* **2016**, *6*, 26781.
[41] E. Aunin, D. Broadley, M. I. Ahmed, A. N. Mardaryev, N. V. Botchkareva, *Sci. Rep.* **2017**, *7*, 3257.
[42] J. Huang, L. Zhao, Y. Fan, L. Liao, P. X. Ma, G. Xiao, D. Chen, *Nat. Commun.* **2019**, *10*, 2876.
[43] Y. Petrenko, I. Vackova, K. Kekulova, M. Chudickova, Z. Koci, K. Turnovcova, H. Kupcova Skalnikova, P. Vodicka, S. Kubinova, *Sci. Rep.* **2020**, *10*, 4290.
[44] C. Harrell, C. Fellabaum, N. Jovicic, V. Djonov, N. Arsenijevic, V. Volarevic, *Cells* **2019**, *8*, 467.
[45] P. T. Newton, L. Li, B. Zhou, C. Schweingruber, M. Hovorakova, M. Xie, X. Sun, L. Sandhow, A. V. Artemov, E. Ivashkin, S. Suter, V. Dyachuk, M. El Shahawy, A. Gritli-Linde, T. Bouderlique, J. Petersen, A. Mollbrink, J. Lundeberg, G. Enikolopov, H. Qian, K. Fried, M. Kasper, E. Hedlund, I. Adameyko, L. Sävendahl, A. S. Chagin, *Nature* **2019**, *567*, 234.
[46] M. Wu, R. Zhang, Q. Zou, Y. Chen, M. Zhou, X. Li, R. Ran, Q. Chen, *Sci. Rep.* **2018**, *8*, 5014.
[47] H. Abe, K. Kamimura, Y. Kobayashi, M. Ohtsuka, H. Miura, R. Ohashi, T. Yokoo, T. Kanefuji, T. Suda, M. Tsuchida, *Mol. Ther. Acids* **2016**, *5*, e276.
[48] D. Xiao, R. Bi, X. Liu, J. Mei, N. Jiang, S. Zhu, *Sci. Rep.* **2019**, *9*, 15596.

[49] U. Iwamoto, H. Hori, Y. Takami, Y. Tokushima, M. Shinzato, M. Yasutake, N. Kitaguchi, *J. Artif. Organs* **2015**, *18*, 315.
[50] W. Wang, D. Rigueur, K. M. Lyons, *Birth Defects Res., Part C* **2014**, *102*, 37.
[51] E. Music, T. J. Klein, W. B. Lott, M. R. Doran, *Sci. Rep.* **2020**, *10*, 8340.
[52] L. Xu, Y. Wu, Z. Xiong, Y. Zhou, Z. Ye, W.-S. Tan, *Sci. Rep.* **2016**, *6*, 1.
[53] H. Liu, X. Jing, A. Dong, B. Bai, H. Wang, *Cell Physiol. Biochem.* **2017**, *44*, 1011.
[54] L. Yang, B. Wang, Q. Zhou, Y. Wang, X. Liu, Z. Liu, Z. Zhan, *Cell Death Dis.* **2018**, *9*, 769.
[55] C. Lu, X. Wang, T. Ha, Y. Hu, L. Liu, X. Zhang, H. Yu, J. Miao, R. Kao, J. Kalbfleisch, *J. Mol. Cell. Cardiol.* **2015**, *89*, 87.
[56] G. Zaccagnini, B. Maimone, P. Fuschi, D. Maselli, G. Spinetti, C. Gaetano, F. Martelli, *Sci. Rep.* **2017**, *7*, 9563.
[57] H. Cheng, S. Chang, R. Xu, L. Chen, X. Song, J. Wu, J. Qian, Y. Zou, J. Ma, *Stem Cell Res. Ther.* **2020**, *11*, 1.
[58] A. B. Aurora, A. I. Mahmoud, X. Luo, B. A. Johnson, E. Van Rooij, S. Matsuzaki, K. M. Humphries, J. A. Hill, R. Bassel-Duby, H. A. Sadek, E. N. Olson, *J. Clin. Invest.* **2012**, *122*, 1222.
[59] A. M. Soliman, S. Das, N. Abd Ghafar, S. L. Teoh, *Front. Genet.* **2018**, *9*, 38.
[60] M. Kurowska-Stolarska, S. Alivernini, L. E. Ballantine, D. L. Asquith, N. L. Millar, D. S. Gilchrist, J. Reilly, M. Ierna, A. R. Fraser, B. Stolarski, *Science* **2011**, *108*, 11193.
[61] N. Magilnick, E. Y. Reyes, W.-L. Wang, S. L. Vonderfecht, J. Gohda, J. Inoue, M. P. Boldin, *Science* **2017**, *114*, E7140.
[62] D. Li, X. I. Li, A. Wang, F. Meisgen, A. Pivarcsi, E. Sonkoly, M. Ståhle, N. X. Landén, *J. Invest. Dermatol.* **2015**, *135*, 1676.
[63] A. Simões, L. Chen, Z. Chen, Y. Zhao, S. Gao, P. T. Marucha, Y. Dai, L. A. DiPietro, X. Zhou, *Sci. Rep.* **2019**, *9*, 7160.
[64] T. Bertero, C. Gastaldi, I. Bourget-Ponzio, B. Mari, G. Meneguzzi, P. Barbry, G. Ponzio, R. Rezzonico, *Cell Death Differ.* **2013**, *20*, 800.
[65] S.-R. Park, J.-W. Kim, H.-S. Jun, J. Y. Roh, H.-Y. Lee, I.-S. Hong, *Mol. Ther.* **2018**, *26*, 606.
[66] V. V. Lunyak, A. Amaro-Ortiz, M. Gaur, *Front. Genet.* **2017**, *8*, 220.
[67] Y.-H. K. Yang, C. R. Ogando, C. W. See, T.-Y. Chang, G. A. Barabino, *Stem Cell Res. Ther.* **2018**, *9*, 131.
[68] I. Rosová, M. Dao, B. Capoccia, D. Link, J. A. Nolta, *Stem Cells* **2008**, *26*, 2173.
[69] S. Sart, T. Ma, Y. Li, *BioRes. Open Access* **2014**, *3*, 137.
[70] C. Hu, L. Li, *J. Cell. Mol. Med.* **2018**, *22*, 1428.
[71] Y. Feng, M. Zhu, S. Dangelmajer, Y. M. Lee, O. Wijesekera, C. X. Castellanos, A. Denduluri, K. L. Chaichana, Q. Li, H. Zhang, A. Levchenko, H. Guerrero-Cazares, A. Quiñones-Hinojosa, *Cell Death Dis.* **2014**, *5*, e1567.
[72] M. Ejtehadifar, K. Shamsasenjan, A. Movassaghpour, P. Akbarzadehlaleh, N. Dehdilani, P. Abbasi, Z. Molaeipour, M. Saleh, *Adv. Pharm. Bull.* **2015**, *5*, 141.
[73] N. E.-M. B. Ahmed, M. Murakami, S. Kaneko, M. Nakashima, *Sci. Rep.* **2016**, *6*, 35476.
[74] L. Liu, J. Gao, Y. Yuan, Q. Chang, Y. Liao, F. Lu, *Cell Biol. Int.* **2013**, *37*, 551.
[75] D. Duscher, E. Neofytou, V. W. Wong, Z. N. Maan, R. C. Rennert, M. Inayathullah, M. Januszyk, M. Rodrigues, A. V. Malkovskiy, A. J. Whitmore, *Science* **2015**, *112*, 94.
[76] J. Flacco, N. Chung, C. P. Blackshear, D. Irizarry, A. Momeni, G. K. Lee, D. Nguyen, G. C. Gurtner, M. T. Longaker, D. C. Wan, *Plast. Reconstr. Surg.* **2018**, *141*, 655.
[77] H. Kang, Y. Yan, P. Jia, K. Yang, C. Guo, H. Chen, J. Qi, N. Qian, X. Xu, F. Wang, *Cell Death Dis.* **2016**, *7*, e2435.
[78] A. Iyer, A. Fenning, J. Lim, G. T. Le, R. C. Reid, M. A. Halili, D. P. Fairlie, L. Brown, *Br. J. Pharmacol.* **2010**, *159*, 1408.
[79] J. P. Cardinale, S. Sriramula, R. Pariaut, A. Guggilam, N. Mariappan, C. M. Elks, J. Francis, *Hypertension* **2010**, *56*, 437.
[80] M. C. Killer, P. Nold, K. Henkenius, L. Fritz, T. Riedlinger, C. Barckhausen, M. Frech, H. Hackstein, A. Neubauer, C. Brendel, *Stem Cell Res. Ther.* **2017**, *8*, 100.
[81] M. François, R. Romieu-Mourez, M. Li, J. Galipeau, *Mol. Ther.* **2012**, *20*, 187.
[82] M. W. Klinker, R. A. Marklein, J. L. Lo Surdo, C.-H. Wei, S. R. Bauer, *Science* **2017**, *114*, E2598.
[83] G. Ren, L. Zhang, X. Zhao, G. Xu, Y. Zhang, A. I. Roberts, R. C. Zhao, Y. Shi, *Cell Stem Cell* **2008**, *2*, 141.
[84] D. D. Ellison, Y. Suhail, J. Afzal, L. Woo, O. Kilic, J. Spees, A. Levchenko, *Science* **2019**, *116*, 14374.
[85] C. Yang, M. W. Tibbitt, L. Basta, K. S. Anseth, *Nat. Mater.* **2014**, *13*, 645.
[86] S. W. Wong, S. Lenzini, M. H. Cooper, D. J. Mooney, J.-W. Shin, *Sci. Adv.* **2020**, *6*, eaaw0158.
[87] Y. Sun, Y. Wang, L. Zhou, Y. Zou, G. Huang, G. Gao, S. Ting, X. Lei, X. Ding, *Sci. Rep.* **2018**, *8*, 2518.
[88] T. J. Bartosh, J. H. Ylöstalo, A. Mohammadipoor, N. Bazhanov, K. Coble, K. Claypool, R. H. Lee, H. Choi, D. J. Prockop, *Science* **2010**, *107*, 13724.
[89] T.-H. Kim, J. H. Choi, Y. Jun, S. M. Lim, S. Park, J.-Y. Paek, S.-H. Lee, J.-Y. Hwang, G. J. Kim, *Sci. Rep.* **2018**, *8*, 15313.v
[90] F. Ezquer, P. Morales, M. E. Quintanilla, D. Santapau, C. Lespay-Rebolledo, M. Ezquer, M. Herrera-Marschitz, Y. Israel, *Sci. Rep.* **2018**, *8*, 4325.
[91] M. Darnell, A. O'Neil, A. Mao, L. Gu, L. L. Rubin, D. J. Mooney, *Proc. Natl. Acad. Sci. USA* **2018**, *115*, E8368.
[92] L. He, M. Ahmad, N. Perrimon, *Exp. Cell Res.* **2019**, *374*, 259.
[93] Y. Wang, C. S. Chen, *J. Cell. Mol. Med.* **2013**, *17*, 823.
[94] A. J. Engler, S. Sen, H. L. Sweeney, D. E. Discher, *Cell* **2006**, *126*, 677.
[95] D. G. Leuning, N. R. M. Beijer, N. A. Du Fossé, S. Vermeulen, E. Lievers, C. Van Kooten, T. J. Rabelink, J. De Boer, *Sci. Rep.* **2018**, *8*, 7716.
[96] T. H. Qazi, D. J. Mooney, G. N. Duda, S. Geissler, *Biomaterials* **2017**, *140*, 103.
[97] A. Uccelli, L. Moretta, V. Pistoia, *Nat. Rev. Immunol.* **2008**, *8*, 726.
[98] A. R. R. Weiss, M. H. Dahlke, *Front. Immunol.* **2019**, *10*, 1191.
[99] K. Németh, A. Leelahavanichkul, P. S. T. Yuen, B. Mayer, A. Parmelee, K. Doi, P. G. Robey, K. Leelahavanichkul, B. H. Koller, J. M. Brown, *Nat. Med.* **2009**, *15*, 42.
[100] H. Kim, M. J. Lee, E.-H. Bae, J. S. Ryu, G. Kaur, H. J. Kim, J. Y. Kim, H. Barreda, S. Y. Jung, J. M. Choi, T. Shigemoto-Kuroda, J. Y. Oh, R. H. Lee, *Mol. Ther.* **2020**, *28*, 1628.
[101] J. Pajarinen, T. Lin, E. Gibon, Y. Kohno, M. Maruyama, K. Nathan, L. Lu, Z. Yao, S. B. Goodman, *Biomaterials* **2019**, *196*, 80.
[102] T. J. Morrison, M. V. Jackson, E. K. Cunningham, A. Kissenpfennig, D. F. McAuley, C. M. O'Kane, A. D. Krasnodembskaya, *Am. J. Respir. Crit. Care Med.* **2017**, *196*, 1275.
[103] A. B. Vasandan, S. Jahnavi, C. Shashank, P. Prasad, A. Kumar, S. J. Prasanna, *Sci. Rep.* **2016**, *6*, 38308.
[104] F. Carty, B. P. Mahon, K. English, *Clin. Exp. Immunol.* **2017**, *188*, 1.
[105] D. M. Patel, J. Shah, A. S. Srivastava, *Stem Cells Int.* **2013**, *2013*, 496218.
[106] J. A. Burdick, R. L. Mauck, S. Gerecht, *Cell Stem Cell* **2016**, *18*, 13.
[107] E. T. Roche, C. L. Hastings, S. A. Lewin, D. E. Shvartsman, Y. Brudno, N. V. Vasilyev, F. J. O'Brien, C. J. Walsh, G. P. Duffy, D. J. Mooney, *Biomaterials* **2014**, *35*, 6850.
[108] T. R. J. Heathman, A. W. Nienow, M. J. McCall, K. Coopman, B. Kara, C. J. Hewitt, *Regener. Med.* **2015**, *10*, 49.
[109] L. Li, X. Chen, W. E. Wang, C. Zeng, *Stem Cells Int.* **2016**, 2016.
[110] L. Kordelas, V. Rebmann, A. K. Ludwig, S. Radtke, J. Ruesing, T. R. Doeppner, M. Epple, P. A. Horn, D. W. Beelen, B. Giebel, *Leukemia* **2014**, *28*, 970.

[111] T. Shigemoto-Kuroda, J. Y. Oh, D. Kim, H. J. Jeong, S. Y. Park, H. J. Lee, J. W. Park, T. W. Kim, S. Y. An, D. J. Prockop, *Stem Cell Rep.* **2017**, *8*, 1214.
[112] R. Zhang, W. Luo, Y. Zhang, D. Zhu, A. C. Midgley, H. Song, A. Khalique, H. Zhang, J. Zhuang, D. Kong, *Sci. Adv.* **2020**, *6*, eaaz8011.
[113] S. Suryaprakash, Y.-H. Lao, H.-Y. Cho, M. Li, H. Y. Ji, D. Shao, H. Hu, C. H. Quek, D. Huang, R. L. Mintz, *Nano Lett.* **2019**, *19*, 1701.
[114] Y. Miyahara, N. Nagaya, M. Kataoka, B. Yanagawa, K. Tanaka, H. Hao, K. Ishino, H. Ishida, T. Shimizu, K. Kangawa, *Nat. Med.* **2006**, *12*, 459.
[115] D. Kim, H. Nishida, S. Y. An, A. K. Shetty, T. J. Bartosh, D. J. Prockop, *Science* **2016**, *113*, 170.
[116] G. E. Salazar-Noratto, G. Luo, C. Denoeud, M. Padrona, A. Moya, M. Bensidhoum, R. Bizios, E. Potier, D. Logeart-Avramoglou, H. Petite, *Stem Cells* **2020**, *38*, 22.
[117] M. Guvendiren, J. A. Burdick, *Curr. Opin. Biotechnol.* **2013**, *24*, 841.
[118] G. Choe, S.-W. Kim, J. Park, J. Park, S. Kim, Y. S. Kim, Y. Ahn, D.-W. Jung, D. R. Williams, J. Y. Lee, *Biomaterials* **2019**, *225*, 119513.
[119] H. Wang, S. C. Heilshorn, *Adv. Mater.* **2015**, *27*, 3717.
[120] K. C. Murphy, S. Y. Fang, J. K. Leach, *Cell Tissue Res.* **2014**, *357*, 91.
[121] G. Feng, Z. Zhang, M. Dang, K. J. Rambhia, P. X. Ma, *Biomaterials* **2020**, *256*, 120213.
[122] K. C. Rustad, V. W. Wong, M. Sorkin, J. P. Glotzbach, M. R. Major, J. Rajadas, M. T. Longaker, G. C. Gurtner, *Biomaterials* **2012**, *33*, 80.
[123] W. Li, Y. Liu, P. Zhang, Y. Tang, M. Zhou, W. Jiang, X. Zhang, G. Wu, Y. Zhou, *ACS Appl. Mater. Interfaces* **2018**, *10*, 5240.
[124] Y. Qin, L. Wang, Z. Gao, G. Chen, C. Zhang, *Sci. Rep.* **2016**, *6*, 21961.
[125] K. Zhang, X. Zhao, X. Chen, Y. Wei, W. Du, Y. Wang, L. Liu, W. Zhao, Z. Han, D. Kong, *ACS Appl. Mater. Interfaces* **2018**, *10*, 30081.
[126] O. P. B. Wiklander, M. Á. Brennan, J. Lötvall, X. O. Breakefield, S. E. L. Andaloussi, *Sci. Transl. Med.* **2019**, *11*, eaav8521.
[127] F. G. Teixeira, K. M. Panchalingam, R. Assunção-Silva, S. C. Serra, B. Mendes-Pinheiro, P. Patrício, S. Jung, S. I. Anjo, B. Manadas, L. Pinto, *Sci. Rep.* **2016**, *6*, 27791.
[128] Z. Zhilai, M. Biling, Q. Sujun, D. Chao, S. Benchao, H. Shuai, Y. Shun, Z. Hui, *Brain Res.* **2016**, *1642*, 426.
[129] G. R. Linares, C.-T. Chiu, L. Scheuing, Y. Leng, H.-M. Liao, D. Maric, D.-M. Chuang, *Exp. Neurol.* **2016**, *281*, 81.
[130] J. M. Santos, S. P. Camões, E. Filipe, M. Cipriano, R. N. Barcia, M. Filipe, M. Teixeira, S. Simões, M. Gaspar, D. Mosqueira, *Stem Cell Res. Ther.* **2015**, *6*, 90.
[131] J. H. Lee, Y.-S. Han, S. H. Lee, *Biomol. Ther.* **2016**, *24*, 260.
[132] L. Xie, M. Mao, L. Zhou, L. Zhang, B. Jiang, *Stem Cells Int.* **2017**, *2017*, 2730472.
[133] A. A. Abdeen, J. B. Weiss, J. Lee, K. A. Kilian, *Tissue Eng., Part A* **2014**, *20*, 2737.
[134] M. E. Ogle, G. Doron, M. J. Levy, J. S. Temenoff, *Tissue Eng., Part A* **2020**. https://doi.org/10.1089/ten.tea.2020.0030.
[135] K. W. Yong, Y. Li, F. Liu, B. Gao, T. J. Lu, W. A. B. W. Abas, W. K. Z. W. Safwani, B. Pingguan-Murphy, Y. Ma, F. Xu, *Sci. Rep.* **2016**, *6*, 33067.

Calvin Chang is a Ph.D. student in the Department of Biomedical Engineering and Translational Tissue Engineering Center at Johns Hopkins University under the supervision of Dr. Hai-Quan Mao. His research focuses on stem cell delivery using biomaterial scaffolds for soft tissue engineering applications.

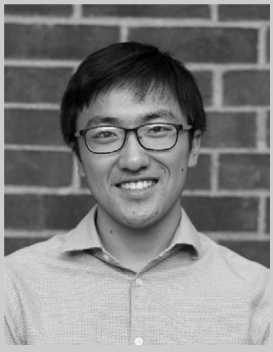

Jerry Yan is a research assistant in Prof. Hai-Quan Mao's lab at the Translational Tissue Engineering Center and Institute for NanoBioTechnology at Johns Hopkins University. His research interests include biomaterials for regenerative medicine and immunoengineering applications.

Zhicheng Yao is a Ph.D. student in the Department of Materials Science and Engineering at the Johns Hopkins University under the guidance of Prof. Hai-Quan Mao. His research interests include designing nanofiber-hydrogel composites for stem cell delivery to repair soft tissue defects. He received his B.E. and M.S.E. degrees in Biomedical Engineering from Zhejiang University.

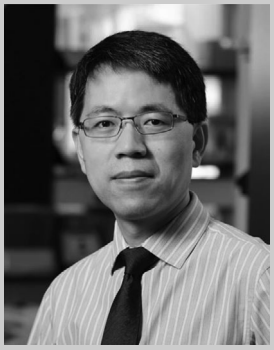

Hai-Quan Mao, Ph.D., is a Professor in Department of Materials Science and Engineering and Department of Biomedical Engineering at Johns Hopkins University, Associate Director of the Institute for NanoBioTechnology, and a faculty member in the Translational Tissue Engineering Center at Johns Hopkins University School of Medicine. His research focuses on development of polymeric biomaterials for regenerative engineering, therapeutic delivery, and immunoengineering applications. He received his B.S. and Ph.D. degrees in polymer chemistry from Wuhan University, and completed his postdoctoral training in the Department of Biomedical Engineering at Johns Hopkins University School of Medicine. He is an Associate Editor for *Biomaterials*.